Optical Biosensors Utilising Viral Receptors ACE2 and ACE2 Mimics

Sian Yang Ow [a], *Laura Sutarlie* [a]*, *Samuel Wei Yang Lim*[a], *Nur Asinah Binte Mohamed Salleh* [a], *Yuki Tanaka*[a], *Chee Kiang Ivan Tan* [a], *Xiaodi Su* [a]*

[a] Institute of Materials Research and Engineering (IMRE), Agency for Science, Technology and Research (A*STAR), 2 Fusionopolis Way, Innovis, #08-03, Singapore 138634, Republic of Singapore

* Corresponding Authors

Email addresses laura-sutarlie@imre.a-star.edu.sg (L. Sutarlie)

xd-su@imre.a-star.edu.sg (X. Su)

Accepted Manuscript

DOI: 10.1016/j.trac.2024.117630

https://doi.org/10.1016/j.trac.2024.117630

ABSTRACT

Numerous viral pathogens can cause pandemics, such as the COVID-19 pandemic caused by the SARS-CoV-2 virus. Rapid diagnosis is critical for timely treatment and for limiting the spread of the disease. Common viral infection starts from binding of the viral pathogens to the viral receptors on the host body, for example, SARS-CoV-2 infects cells by binding to human angiotensin converting enzyme 2 (ACE2) using the virus S protein and can be exploited for biosensor development. This review discusses optical biosensors that exploit ACE2 or ACE2 derived peptides (ACE2 mimics) as an affinity ligand for detecting SARS-CoV-2. In these ACE2- and ACE2-mimics-based optical biosensors, the target analytes can include whole virus (surrogate pseudoviruses and inactivated SARS-CoV-2 virus), spike proteins (S protein), or receptor binding domain (RBD) of the S protein. The optical transducer formats include lateral flow assays, colorimetric assays, fluorimetric assays, surface enhanced Raman spectroscopy, localised surface plasmon resonance etc. The sensor performances (such as limit of detection and turnover time) was compared among various optical biosensor formats. We highlight the advantages of using ACE2 and/or ACE2 mimics over common affinity ligands (such as antibodies) against future virus mutations. We also discussed the advantages of the smaller sized ACE2 mimics relative to ACE2 protein for achieving more versatile optical sensor designs involving nanomaterials and higher selectivity to SARS-CoV-2. In addition to SARS-CoV-2 detection, this review also discusses the expanded application of ACE2-based optical biosensors for the detection of non-viral targets, e.g., SARS-CoV-2 neutralising antibodies and anti-SARS-CoV-2 drugs.

Keywords:

Optical biosensors; angiotensin converting enzyme 2; viral receptor; lateral flow; colourimetric biosensor; fluorimetric biosensor; surface enhanced Raman spectroscopy; localised surface plasmon resonance biosensor; SARS-CoV-2 biosensor; neutralising antibody biosensor.

Abbreviations:

ACE2: angiotensin converting enzyme 2

ACE2 mimic: Peptides derived from the binding site of ACE2 to the SARS-CoV-2 spike protein

Ag-RDT: Antigen rapid diagnostic tests

APTES: (3-Aminopropyl) triethoxysilane

AuNP: Gold Nanoparticles

ART: Antigen rapid test

BHQ2: black hole quencher 2

BSL: Biosafety level

EDC: 1-ethyl-3-(-3-dimethylaminopropyl) carbodiimide

FRET: Fluorescence resonance energy transfer

K_d: Dissociation constant

LOD: Limit of detection

LSPR: Localised surface plasmon resonance

N protein: Nucleocapsid protein

NHS: N-hydroxysuccinimide

PBS: Phosphate buffered saline

PCR: Polymerase Chain Reaction

PEG: polyethylene glycol

PFU: Plaque forming unit

RBD: Receptor-binding domain

RT-PCR: Real-time Polymerase Chain reaction

S protein: Spike protein

SARS-CoV-1: Severe acute respiratory syndrome coronavirus 1

SARS-CoV-2: Severe acute respiratory syndrome coronavirus 2

SERS: Surface enhanced Raman spectroscopy

SPR: Surface plasma resonance

SWCNT: single wall carbon nanotubes

$TCID_{50}$: 50% tissue culture infectious dose

TMB: 3,3', 5,5'-tetramethylbenzidine

Graphical Abstract

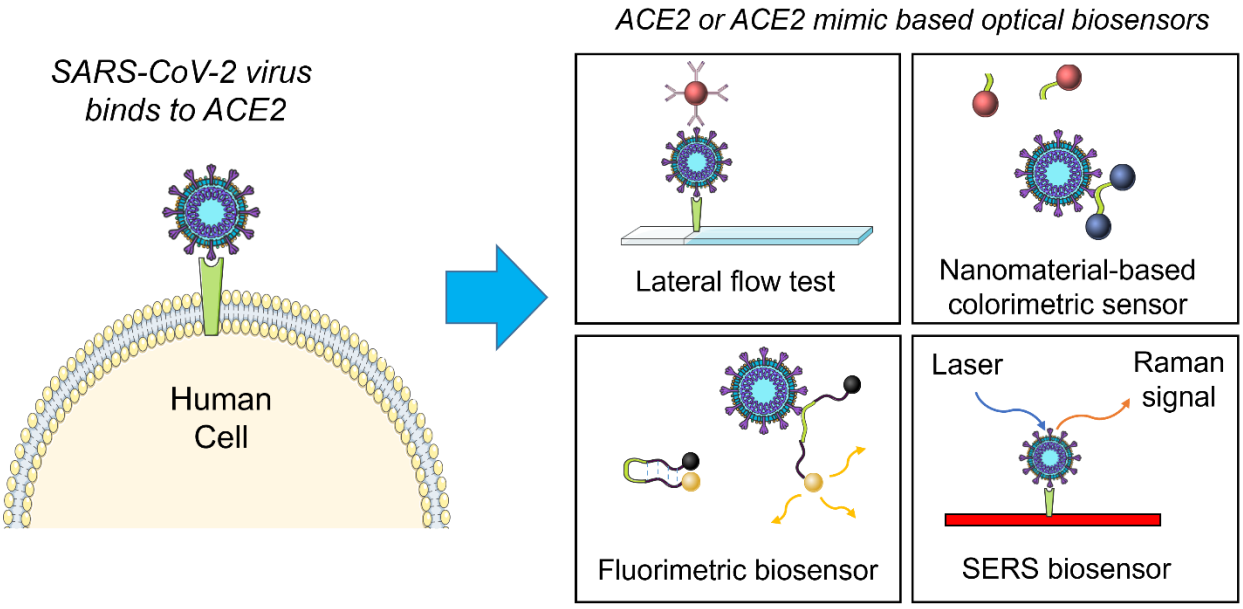

Image was partially generated using Servier Medical Art, provided by Servier, licensed under a Creative Commons Attribution 3.0 unported license https://creativecommons.org/licenses/by/3.0/. Adaptations of “Receptors 1”, “Receptors 2” and “SARS- CoV-2” from Servier Medical Art were used in the creation of this image.

1. Introduction

SARS-CoV-2 is a β- coronavirus that caused the global pandemic of Coronavirus Disease 2019 or COVID-19. SARS-CoV-2 is a typical ~ 91 nm diameter spherical [1] membrane bound coronavirus covered with three main transmembrane proteins: a large protein complex known as the spike or S protein, a smaller envelope or E protein and a membrane/matrix protein or M protein [2]. SARS-CoV-2 infects cells by binding with the host cell's angiotensin converting enzyme 2 (ACE2) via the S protein's receptor binding domain (RBD).

Initially, diagnosis of COVID-19 was achieved on a large scale using laboratory-based PCR to detect the viral RNA from nasal swabs [3]. Over time, lateral flow COVID-19 diagnostics kits, also known as the 'Antigen Rapid Test' (ART) kits or 'Antigen Rapid Diagnostic Tests' (Ag-RDT) [4, 5] have been emerged for point-of-care diagnosis. These kits typically target the N protein of SARS-CoV-2 [6] and produce results within 15-30 minutes. However, they have a lower analytical sensitivity (LOD of $10^6 – 10^7$ copies/ml) [7] as compared to existing RT-PCR kits (LOD of 10^2- 10^3 copies/ml) [3]. Despite the lower sensitivity, they are still able to detect the vast majority of COVID 19 cases as the peak viral load in infected people is typically above the LOD of most ART kits [8].

Optical biosensors are devices that use optical signals to detect an analyte with the aid of biological sensing components or affinity ligands [9]. The sensing components (e.g. antibodies, aptamers, or antigens) interact with respective target analyte (e.g. whole virus, viral antigen, or virial RNA) to generate a detectable optical signals in the form of coloured lines in lateral flow test, shifts in surface plasmon resonance (SPR) angle, change in localised SPR (LSPR), surface enhance Raman spectroscopy (SERS), colorimetric change or fluorescent emission, etc [10]. In optical biosensors for SARS-CoV-2 S protein antigen or virus particles, antibodies are commonly

used as bioaffinity ligands. While antibodies are typically specific to the virus, new strains of SARS-CoV-2 exhibit decreased affinity to some existing antibodies [11] and can affect the sensitivity of antibody-based biosensors. As all currently known strains of SARS-CoV-2, such as omicron BA2, still utilize ACE2 to enter the host cell [12, 13], the use of ACE2 as the receptor effectively futureproofs the sensor against future mutations of the virus.

In this review, we discuss optical biosensors that use ACE2 protein and ACE2 mimics (i.e., peptides derived from ACE2 that bind to SARS-CoV-2 S protein) for the detection of SARS-CoV-2 virus, antigens, neutralising antibodies and inhibitor drugs. While a number of reviews on SARS-CoV-2 biosensors have been published [14-16], including those focusing on optical sensors (e.g. colorimetric SARS-CoV-2 nanosensors [17] and nanophotonic biosensors for identifying SARS-CoV-2 variants [18]) and ACE2-based biosensors [19, 20], here we further expand the knowledge on the use of both ACE2 and ACE2 mimics for optical biosensor development. We start by introducing ACE2 receptor and ACE2 mimics. We then describe various viral surrogates that have been used for the construction and validation of the SARS-CoV-2 biosensors. After that, we discuss the various ACE2- and ACE2 mimic-based optical biosensors for their principles and extended applications not only for SARS-CoV-2 detection, but also for the detection of non-viral targets (e.g., SARS-CoV-2 neutralising antibodies and anti-SARS-CoV-2 drugs). Finally, we compare the advantages and limitations of using ACE2 protein and ACE2 mimics and the related performance of the various optical biosensors. We also provide some perspective into the clinical viability and other applications from an analysis of the performance of these biosensors.

2. ACE2 protein and ACE2 mimics

ACE2 normally exists as a homodimer and serves as a receptor for several viruses to enter cells, most notably SARS-CoV-2, SARS-CoV-1 and NL63. Although ACE2 is a transmembrane enzyme, it also exists in a soluble form after the ACE2 transmembrane domain is cleaved various enzymes [21]. Fig. 1 shows the full structure of ACE2 that consists of four main domains, namely the signalling peptide, soluble extracellular domain, transmembrane domain, and cytoplasmic domain.

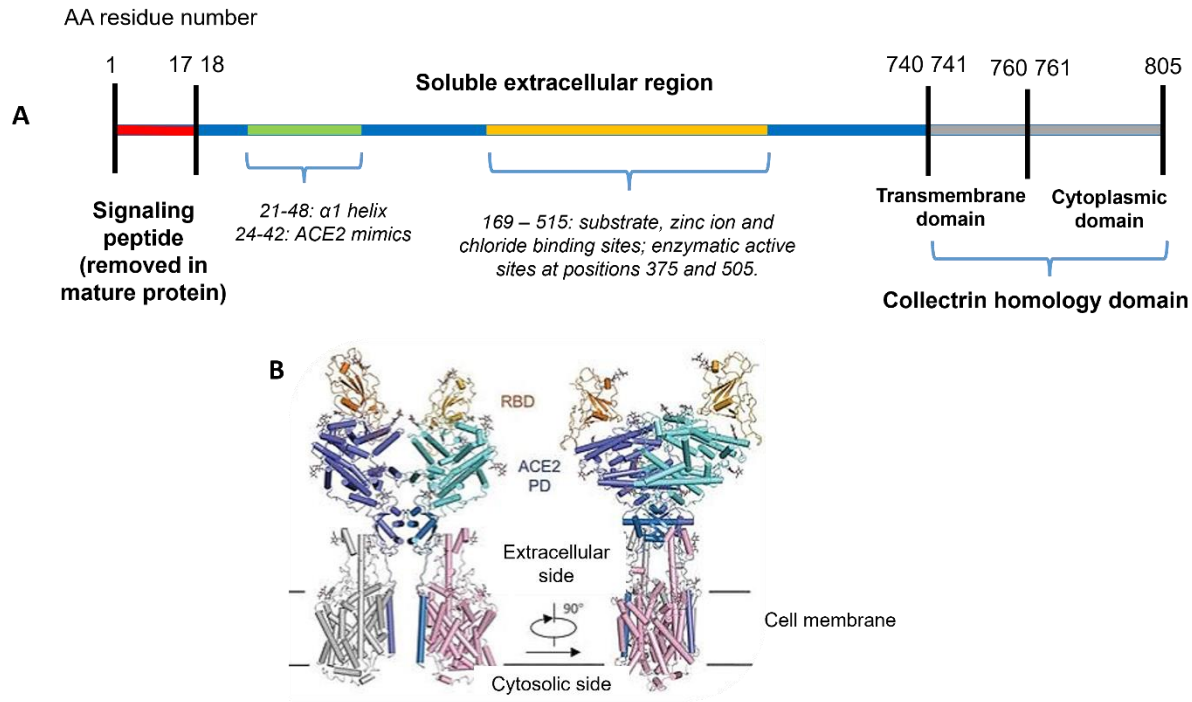

Fig. 1. (A) The unfolded ACE2 protein showing the location of the four domains on the protein, as well as the location of the SARS-CoV-2 ACE2 mimics and the region involved in the enzyme substrate-binding site based on Uniprot accession number Q9BYF1. (B) 3D representation of the complete folded ACE2 protein dimer on a cell membrane, as well as the attachment point of the SARS-CoV-2 RBD Image taken from Ref. [22], reproduced under a Creative Commons Attribution License 4.0 (CC BY) https://creativecommons.org/licenses/by/4.0/ .

The normal enzymatic function of ACE2 is to convert angiotensin 1 and angiotensin 2 to angiotensin 1-9 and 1-7, respectively, as part of the renin-angiotensin system [21]. The active site of ACE2, i.e. residues 375 and 505 in the soluble extracellular domain, is not involved in the

binding of SARS-CoV-2 virus and the binding of ACE2 inhibitors does not affect the binding of ACE2 to SARS-CoV-2 S protein [23]. Instead, the SARS-CoV-2 S proteins bind to a region near the N terminus, known as the α1 helix [22, 24].

The fact that SARS-CoV-2 S protein mainly recognises a region of ACE2 in the soluble extracellular domain near the N terminus (the α1 helix) has led to the exploration of using truncated ACE2 peptides (termed as ACE2 mimics) for various applications, such as a SARS-CoV-2 virus binding inhibitors [25]. These same ACE2 mimic peptides can be used for capturing the S protein or the virus in the development of SARS-CoV-2 biosensors [24]. The majority of ACE2 mimics for optical biosensor development are based on the N terminal amino acid (AA) residues 24-42 as the core [24, 26-28].

3. Viral surrogates used in ACE2- and ACE2 mimics-based optical biosensors

SARS-CoV-2 requires biosafety level 3 (BSL3) handling facilities [29], which is not easily available. Thus, various viral surrogates are involved in the biosensor development, including inactivated viruses, *pseudoviruses* and viral proteins. For example, ACE2-based optical biosensors were developed against SARS-CoV-2 S protein, S1 subunit, or RBD [30-33]. However, recombinant S proteins from different cell lines may exhibit different binding affinity to ACE2 [34]. Furthermore, recombinant proteins are significantly smaller than the whole virus, which may result in differences in biosensor performance as compared to biosensors tested with whole viruses.

Pseudoviruses are also commonly used as a safer analogue to the SARS-CoV-2 virus for biosensor development. Some pseudoviruses are made by modifying other viruses (e.g. vesicular stomatitis virus) to produce the viral receptor protein of interest (e.g. S protein) [29]. *Pseudoviruses* can also be made by inserting plasmids encoding the relevant viral proteins into cells to produce

pseudovirus particles, and was used to validate a fluorescence ACE2 mimic-based biosensor [26] and a SERS ACE2-based biosensor [35]. *Pseudoviruses* can infect cells in a similar manner to SARS-CoV-2 viruses and require a lower biosafety level at biosafety level 2 (BSL2) [29]. However, *pseudoviruses* may interact differently with the receptor compared to SARS-CoV-2 virus due to the structural differences. For example, vesicular stomatitis virus is bullet-shaped [36], while SARS-CoV-2 is spherical [1].

Inactivated SARS-CoV-2 viruses can also be used for biosensor testing. For example, heat inactivated SARS-CoV-2 virus was used to validate a SERS based biosensor [37]. While safer than using viable SARS-CoV-2 viruses for biosensor testing, excessively harsh inactivation methods can denature the S proteins and interfere with binding assays studies. In view of the different physiological, structural, and biochemical properties of the various surrogate analytes, their impact on sensor performance will be discussed in Section 7.

4. ACE2-based optical biosensors for the detection of SARS-CoV-2

Soluble recombinant ACE2 (residues 18-740) is most often used for the construction of ACE2-based biosensors as it is easy to handle in aqueous media and is commercially available. Table 1 shows a summary of the targets and performance of the various ACE2-based optical biosensors. Protein LODs were converted to nM to better compare LODs based on number of protein molecules detected.

Table 1. SARS-CoV-2 optical biosensors that utilise soluble ACE2 as affinity ligand [a]

No.	ACE2 type	Detection Principle	Target (MW)	LOD [b]	Sensitivity | Selectivity | Accuracy | Sample	Assay time	Ref.
1	Soluble extracellular	Lateral flow	S1 (76.5 kDa)	5 ng/ml (6.54×10^{-2} nM)	NA***	20 min	[38]
			Clinical virus samples	5.35×10^{6} copies/ml			
2	Soluble extracellular	Lateral flow	Wild type S1 (76.5 kDa)	10 ng/ml S1 (0.131 nM)	NA	20 min	[30]
			Wild type RBD (26.6 kDa)	2 ng/ml (0.0752 nM)			
3	Soluble extracellular	Colorimetric	S protein*	1.54×10^{-4} ng/ml (1.15×10^{-6} nM)	96% | 94% | 90% | 100 Clinical samples	5 min	[31]
4	Soluble extracellular	Colorimetric	S protein (37 kDa)	4.98 ng/ml (0.116 nM)	97.56% | 90.24% | 93.90% | 600 Clinical samples	30 min	[32]
5	Soluble extracellular	Fluorescence	RBD*	12.6 nM (33.44 ng/ml)	NA | 70.07% | NA | SARS-CoV-1, SARS-CoV-2, MERS S protein, and	90 min	[33]

					various other proteins		
6	Soluble extracellular	SERS	S protein* Pseudovirus	1.77× 10^{-2} nM (2.38 ng/ml) 80 copies/ml	80 copies/ml | NA | NA | water samples	5 min	[35]
7	Not Stated	SERS	Inactivated SARS-CoV-2	66 copies/ml	NA | NA | 100% | 100 simulated throat and nasal swabs	15 min	[37]
8	Not Stated	SERS	S Protein*	4.5 × 10^{-6} ng/ml (3.62 × 10^{-8} nM)	NA	~15 min	[39]
9	Engineered Trimeric ACE2	LSPR	Inactivated SARS-CoV-2	100 $TCID_{50}$/ml	NA	5 min (single sample)	[40]
10	Soluble extracellular	LSPR	RBD (26.54 kDa) NL63 Virus	8.3 × 10^{-4} nM (0.0220 ng/ml) 391 PFU/ml**	NA	< 20min	[41]
11	Soluble extracellular	Localised refractive index changes	S Protein (134.36 kDa)	8.49 ng/ml (6.32 × 10^{-2} nM)	NA	3 min	[42]

[a] *Unless otherwise stated, pseudoviruses, RBD, S1 and S protein in this table refer to that from SARS-CoV-2. SERS refers to Surface enhanced Raman Spectroscopy; LSPR refers to Localised Surface Plasmon Resonance. Concentration values in brackets were converted from values listed in the cited paper. Where multiple LODs were stated for different background matrices, the lowest was quoted in the table. b. the LOD values in brackets were converted from the reported LOD values using the MW of the respective proteins. *S protein MW was not available or stated so conversion from molar to mass concentrations assumed a 134.36 kDa MW of for S protein and 26.54 kDa for RBD. **PFU = Plaque forming units. *** NA = data unavailable.*

4.1. Lateral flow sensors of SARS-COV-2 utilising soluble ACE2.

Lateral flow assay kits typically consist of a sample pad, conjugate pad (or releasing pad), a detection pad (nitrocellulose membrane) and an absorbent pad. The sample solution is added to the sample pad and flows towards the conjugate pad and reacts with affinity ligand-functionalised probes [43, 44]. Any analyte conjugated probe then binds to and forms a sandwich complex with the capture antibody/receptor on the test line [6, 30]. This results in the appearance of a signal, such as a coloured line, fluorescent line or SERS signal [44]. A control line with a capture antibody reactive to the affinity ligand on the probe is stained by the excess probe to show that the strip operates correctly [45]. These assays are capable of detecting attomolar concentrations of RBD [46] and are a popular choice for optical biosensors as they are inexpensive, easy to use, often require no additional equipment for operation and give results in 5-30 minutes. [45, 47].

Instead of using a pair of antibodies, ACE2 and a suitable antibody can form the pair to sandwich the analyte in lateral flow test for COVID-19 (Figure 2A). Using a detection probe of anti-S1 IgG-conjugated red cellulose nanobeads in the conjugate pad and ACE2 printed on the test line [30, 38], a LOD of < 5 ng/ml (0.0654 nM) of SARS-CoV-2 S1 protein [38] or 10 ng/ml (0.131 nM) SARS-CoV-2 S1 protein [30] was achieved with this set up. When tested with cultured clinical viral samples, these sensors could reach a LOD of 5.35×10^6 copies/ml [38], which is similar to the $10^5 – 10^7$ copies/ml reported for commercial ART kits [7, 26]. The lateral flow sensor that reported the 10 ng/ml (0.131 nM) LOD for SARS-CoV-2 S1 protein also reported a LOD of 2 ng/ml (0.0752 nM) for RBD. The lower LOD (higher sensitivity) to RBD was attributed to the lower K_d values of the same antibody to RBD (K_d = 4.16 nM) as compared to S1 (K_d = 17.02 nM) reported in the same reference using biolayer interferometry (BLI) [30]. It is worth noting that K_d values were typically calculated by dividing the measured association and disassociation rates of

the analyte and receptor, often measured using SPR or BLI. As the association between RBD and ACE2 is reported to have heterogeneous interactions, care must be taken in the calculation of the K_d values of RBD and ACE2 using the software provided with SPR or BLI equipment assuming a single step reaction [48]. Despite such potential inaccuracy, we believe the K_d reported by the same method holds a valid comparison of relative affinity, which is key contributor to the difference in sensor sensitivity. The use of ACE2 instead of a capture antibody allows for easier selection of the probe antibody by selecting a non-neutralising or non-RBD binding antibody. Incorrectly paired antibodies may result in false positives if the antibodies bind to each other or give false negative results if their epitopes overlap, as observed in a lateral flow sensor [38].

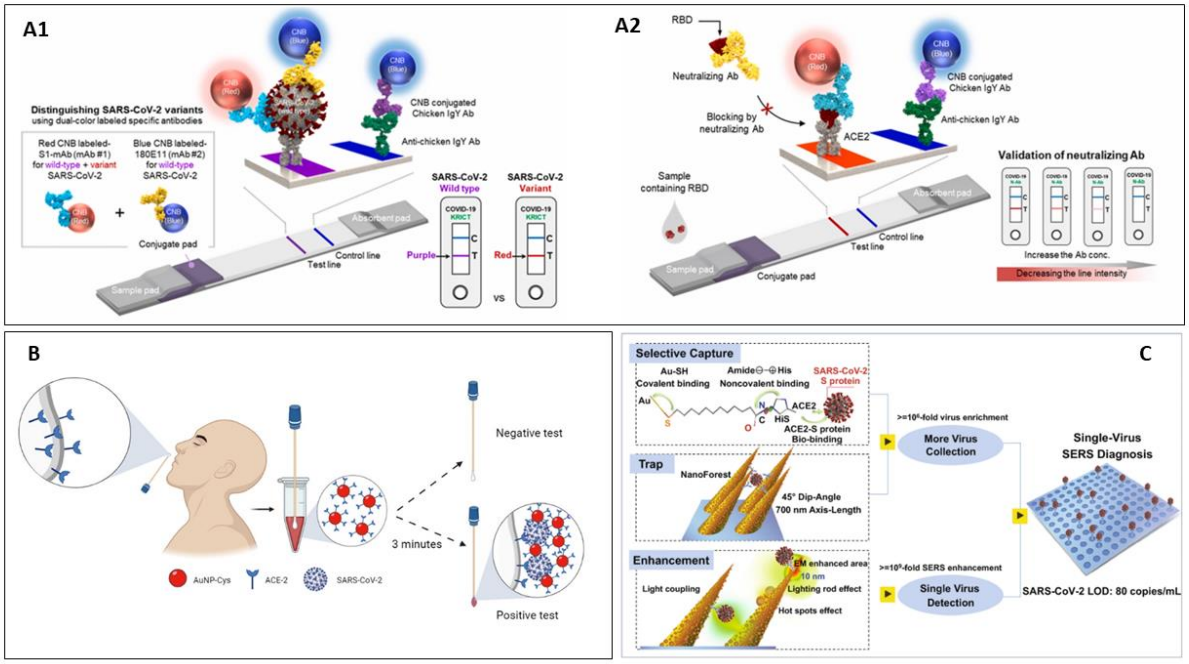

Fig. 2. (A1 and A2) A dual-use ACE2-based lateral flow biosensor setup capable of differentiating (A1) SARS-CoV-2 strains and (A2) SARS-CoV-2 neutralising antibodies [30], Image was adapted from figures in Ref. [30], under a Creative Commons CC-BY licence https://creativecommons.org/licenses/by/4.0/. (B) A colorimetric swab based biosensor for SARS-CoV-2 [31]. Reprinted (adapted) with permission from Ref. [31], *ACS Nano* 2021, 15, 11, 17453-17462. Copyright 2021 American Chemical Society. (C) A SARS-CoV-2 SERS biosensor that utilizes machine learning for detection of the virus [35]. Figure used without modification from

Ref. 84, licensed under a Creative Commons Attribution 4.0 International License http://creativecommons.org/licenses/by/4.0/.

ACE2-based lateral flow systems can be modified to include other functionalities, such as SARS-CoV-2 variants identification using two anti-SARS-CoV-2 S1 antibodies that have differential affinity to different SARS-CoV-2 strains conjugated with either red or blue cellulose nanobeads (Figure 2A1) [30]. The strain identity can be determined by the intensity of the red and blue staining on the test strip, using a portable line analyser. Furthermore, the same lateral flow sensor can also be modified to detect neutralising antibodies (Fig. 2A) and this would be discussed in further detail in Section 6.

4.2. Nanoparticle-based colorimetric and fluorimetric sensors for SARS-CoV-2 utilising soluble ACE2.

Optical biosensors can be built exploiting various nanoparticles, including gold nanoparticles (AuNPs) that change colour on aggregation [17, 49]. In an ACE2- and AuNP-based design, ACE2-functionalised cotton swabs firstly captured the virus (S protein) from patient nasal swab samples, after which the swabs were immersed into an ACE2-AuNP conjugate solution [31]. As the S protein is trimeric [50], it acts as a cross linker to aggregate ACE2-AuNPs on the swabs due to the formation of ACE2-S-ACE2 sandwiched complex. The resulting purple stain on the swabs allow for infection detection within 5 minutes at a LOD of 0.154 pg/ml (for the S protein). From 100 nasopharyngeal/oropharyngeal (NP/OP) clinical samples, the method shown a 96% sensitivity and 90% accuracy.

Metal-bearing nanoparticles can also be used to catalyse a colour change in an optical biosensor. For instance, γFe_2O_3 nanoparticles catalyse the oxidation of 3,3′,5,5′-

tetramethylbenzidine (TMB) solution in the presence of H_2O_2 to produce a blue-coloured oxidised TMB solution. The presence of SARS-CoV-2 S protein bound to soluble ACE2 causes the blue coloured oxidised TMB solution to turn colourless in 30 minutes, with LOD of 4.98 ng/ml when quantified via absorbance measurements [32]. It is believed that the binding of S protein to ACE2 results in the stressing of the disulfide bond of the S protein [32, 51], exposing the cysteine residues of the disulfide bonds which reduce the blue oxidized TMB solution into a colourless solution [32].

Fluorescence biosensors using ACE2 are also possible. For example, using ACE2-functionalised single wall carbon nanotubes (SWCNT) that increase near-infrared fluorescence when SARS-CoV-2 RBD binds to it. This achieved an LOD of 12.6 nM in 90 min incubation for RBD. Additionally, the sensor was insensitive to biological contaminants, due to the use of near-infrared fluorescence [33].

4.3 SERS, LSPR and other optical coronavirus biosensors utilising soluble ACE2.

SERS relies on noble metal nanostructures or nanoparticles to create a localised electric field on laser excitation to enhance the weaker Raman signals from analytes. In general, there are two modes of SERS sensing: i) direct mode and ii) indirect mode. In direct mode, the intrinsic Raman signatures of the analyte is used, and are often coupled with machine learning to aid spectrum analysis. In indirect mode, the Raman signatures of a reporter molecule bound to the SERS substrate is used instead [52]. While SERS can detect trace quantities of analyte by identifying their signature Raman fingerprints, it is prone to interfering signals from other contaminants [35].

A SERS-based SARS-CoV-2 biosensor was reported to use ACE2 conjugated to magnetic molybdenum trioxide-polydopamine-gold functionalised nanospheres to magnetically concentrate SARS-CoV-2 S protein onto a silicon substrate for measurement via a Raman confocal microscope, achieving a LOD of 4.5 fg/ml S protein [39]. SERS signals from analytes also can be enhanced by the use of nanostructures such as the hot spots between adjacent gold spikes and sharp tips in gold nano-spike arrays [35]. An ACE2 conjugated gold nano-spike array coupled with Raman spectrum interpretation via machine learning was reported to achieve a detection of 80 copies/ml of pseudovirus in 5 minutes of sample incubation (Figure 2C) [35]. The SERS enhancement using gold nano-spike arrays can be further enhanced with magnetic enrichment using ACE2 conjugated Fe_3O_4-Au composite nanoparticles achieving a LOD of 66 copies/ml of SARS-CoV-2 virus from nasal and throat swabs in 15 min [37].

Noble metal nanoparticles exhibit LSPR, which refers to the collective oscillation of electrons upon interaction with light [53] which can change due to molecular interactions, resulting in LSPR peak shifts suitable for use in LSPR biosensors [40, 41]. Two examples of ACE2-conjugated LSPR sensors for SARS-CoV-2 use ACE2 conjugated on titanium and gold coated porous silicon [40], or a silver nanotriangle array, where the ACE2 was conjugated via electrostatic and hydrophobic interactions [41]. The porous silicon LSPR biosensor had a LOD of 100 $TCID_{50}$ SARS-CoV-2 virus and 10^7 copies/ml pseudovirus from culture media in 5 min [40], while the nanotriangle array had a LOD of 0.83 pM SARS-CoV-2 RBD in dilution buffer (modified PBS) and 625 PFU/ml of NL63 in saliva [41].

The localised refractive index of fibre optic cables have also been used for SARS-CoV-2 biosensors [42]. ACE2 was immobilised on a slightly tapered no-core glass fibre, via 1-ethyl-3-(-3-dimethylaminopropyl) carbodiimide (EDC) and Sulfo-NHS (*N*-hydroxysuccinimide) coupling

after glutaraldehyde treatment of the (3-Aminopropyl) triethoxysilane (APTES) salinised glass fibre. The binding of S protein to the ACE2 results in changes in the refractive index of the fibre, and shifts in wavelength of the light passing through the cable achieving a LOD of 8.49 ng/ml for the S protein (124.36 kDa) in PBS within 3 minutes [42].

4.4. Limitations of ACE2-based optical biosensors

A major limitation of ACE2 based biosensors for the specific detection of SARS-CoV-2 viruses is the cross-reactivity with other viruses and biomolecules, such as SARS-CoV-1 and the common cold coronavirus NL63 [54]. The affinity of ACE2 to SARS-CoV-2 is slightly higher (K_d 4.63×10^{-8} M) [55] than that to SARS-CoV-1 (K_d 8.71×10^{-8} M) [56] and about 10 - 100 times higher than that of NL63 S protein [56, 57]. However, NL63 is also detectable by ACE2-based SERS biosensors [41]. Furthermore, biomolecules commonly present in patient samples, such as angiotensin, can bind to ACE2 in the 169-515 region of the protein (uniprot entry Q9BYF1) [58] and result in false positive results. Additional affinity receptors such as SARS-CoV-2 specific antibodies [38] or other identification methods, such as SERS fingerprinting [35], can be used together with the ACE2 to mitigate the abovementioned false positives. Alternatively, this non-specificity can be mitigated by using ACE2 mimics instead of whole ACE2 [27].

5. ACE2 mimics-based optical biosensors for detection of SARS-CoV-2

There are several advantages in using short ACE2 peptide mimics over the full ACE2 protein for biosensors. Firstly, the short peptides allow for the design of biosensors that are not possible using the much larger ACE2 protein, such as the creation of molecular beacon FRET probes [26]. Secondly, although small peptides are still susceptible to pH and buffer changes [59],

they are more tolerant to chemicals and resistant to denaturation than larger proteins. Lastly, ACE2 derived peptide mimics may confer higher specificity to SARS-CoV-2 [27] in comparison to whole ACE2. This is because the RBD binding involves different AA residues of ACE2 for the SARS-CoV-2, SARS-CoV-1 [60] and with NL63 [61] and also lack the ACE2 substrate binding site. Table 2 summarises the analyte target and sensor performance for SARS-CoV-2 biosensors that utilise ACE2 peptide mimics. Selectivity and sensitivity data was not available for any of the papers in Table 2.

Table 2. SARS-CoV-2 optical biosensors using ACE2 mimics as affinity ligand

N.o	ACE2 Residues	Detection principle	Target (MW)	LOD	Assay time	Ref.
1	MYGGG- (24-30) (34-41)-GGKGDF	Colorimetric	RBD (26.3kDa) lysed pseudovirus	0.01 nM (26.3 ng/ml) 10^5 copies/ml	< 30 min	[62]
2	(21 – 48) - K	Fluorescence	RBD (26.54 kDa)	0.0525 nM (0.139 ng/ml)	60 – 240 min	[24]
3	Binding peptide - CFN - (26 – 46) – binding peptide	Fluorescence	RBD (29 kDa) Pseudovirus	7.00×10^4 nM (2.03×10^{-3} ng/ml) 10^5 copies/ml	10 min	[26]
4	21 - 43	SERS	S protein (134.36 kDa)	300 nM (4.03×10^4 ng/ml)	~30 min	[27]

Conversion of LOD of the S/S1/RBD protein was performed for articles where the manufacturer provided the MW. LOD values in ng/ml in brackets were converted from the published LOD values.

5.1. Nanoparticle-based colorimetric and fluorimetric sensors of SARS-COV-2 utilising ACE2 mimics.

An AuNPs-based colorimetric sensor was designed with two AuNPs each conjugated with a different half of an ACE2 mimic peptide work (Figure 3A) [62]. The two halves bind to different parts of the S protein RBD, allowing the RBD to crosslink and aggregate the conjugated AuNPs, causing a change in colour. A LOD of 0.01 nM was reported for S Protein RBD and 10^5 copies of lysed SARS-CoV-2 pseudovirus [62].

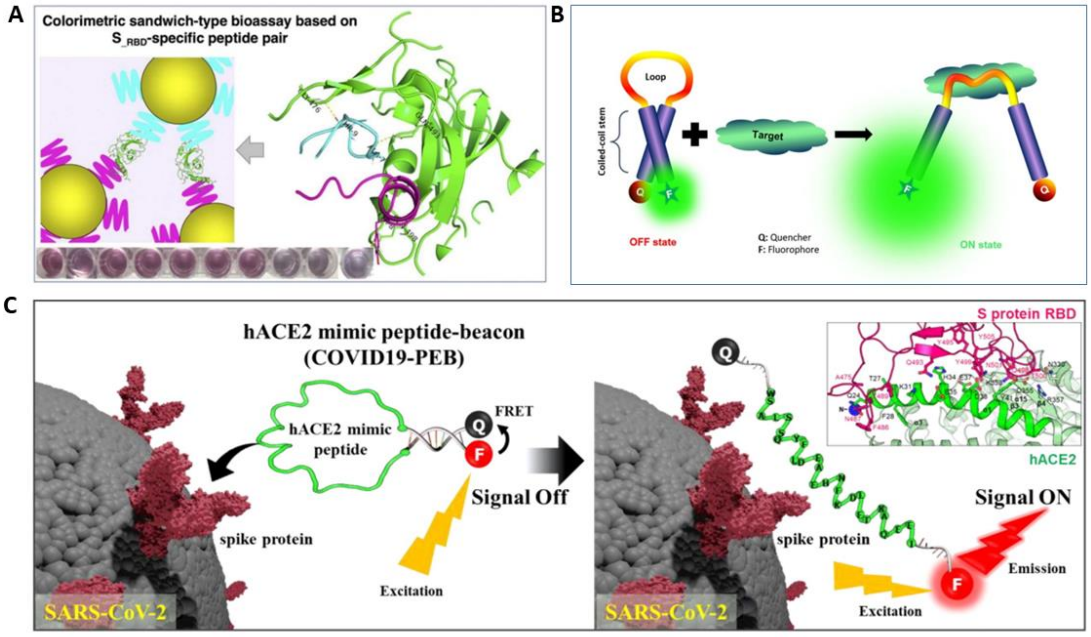

Fig. 3: (A) A nanoparticle aggregation based biosensor using two halves of an ACE2 mimic peptide [62], image from Ref. [62] reprinted from *Journal of Hazardous Materials* **425**, Zhu, Q. & Zhou, X, A colorimetric sandwich-type bioassay for SARS-CoV-2 using a hACE2-based affinity peptide pair, Page number 127923, copyright (2022), with permission from Elsevier. (B) ACE2 receptor mimic FRET probe design using complimentary coiled-coil peptides, showing the probe without target and when bound to a target [26], image from Ref. [26] reproduced under a Creative Commons Attribution License 4.0 (CC BY NC) https://creativecommons.org/licenses/by-nc/4.0/. (C) ACE2 receptor mimic FRET probe design using complimentary DNA showing the probe conformation before and after binding to SARS-

CoV-2 spike protein [24], image from Ref [24] used with permission under the Creative Commons CC-BY-NC-ND licence.

Fluorescence resonance energy transfer (FRET) is a popular phenomenon for biosensor design where the fluorescence of a fluorophore is quenched when in close proximity to the quencher [24]. FRET based biosensors probes have been developed where each side of the ACE2 mimic peptide was modified with a fluorophore and a quencher. In one example, both terminus of the ACE2 mimics were conjugated with complimentary DNA oligonucleotide with A CY3 fluorophore or a black hole quencher 2 (BHQ2) on at each oligonucleotide terminus (Figure 3C) [24]. An alternative design used a "coiled-coil peptide probe design", where a fluorophore and quencher conjugated to a pair of α-helical peptides that self-assemble into a super helix (Figure 3B) [26]. In both designs, complimentary DNA binding or super-helix formation causes the ACE2 receptor mimic to bend into a hairpin shape, bringing the terminal fluorophore and quencher pairs into close proximity and quenching the fluorescence signal. Binding of SARS-CoV-2 S protein to the ACE2 mimic section dehybridises the complimentary DNA helix or opens the coiled-coil peptide respectively, resulting in fluorescence recovery as a light-on sensor. The DNA FRET probe sensor reported a LOD of 52.5 pM for SARS-CoV-2 S protein [24], while the coiled-coil probe design reported a LOD of 700 aM of SARS-CoV-2 RBD and 10^5 Copies/ml of SARS-CoV-2 pseudovirus using a miniaturised total internal reflection microscope [26].

5.2. SERS sensors of SARS-CoV-2 utilising ACE2 mimics.

The use of small peptides is advantageous for SERS based biosensors as large protein molecules produce their own interfering SERS spectra [27]. An example of this approach uses a cysteine-PEG (polyethylene glycol) modified ACE2 mimic attached to a nanostructured gold

substrate [27]. The resulting Raman intensity changes of the spectrum on laser excitation was analysed using multivariate curve analysis (MCR) to give a LOD of 300 nM for SARS-COV-2 S protein. The peptide was found to be more specific to the SARS-COV-2 S protein over the S protein from SARS-COV-1 and MERS-COV [27] as compared to whole ACE2 protein.

6. Optical biosensors utilising ACE2 for non-viral targets

While many biosensors utilising ACE2 or ACE2 mimics were intended for the detection of SARS-CoV-2, ACE2 optical biosensors can also be configured for the detection of SARS-CoV-2 neutralising antibodies and antiviral drugs. The details of these sensors are summarised in Table 3. Selectivity and sensitivity data was unavailable for all entries in Table 3.

Table 3. ACE2-based optical biosensors for detection of neutralising antibodies and drug candidates

N.o	ACE2 domain	Detection principle	Intended target	Assay Time	Ref.
1	Soluble Extracellular	Lateral flow	SARS-COV-2 neutralising antibodies	20 min	[30]
2	Soluble Extracellular	Lateral flow	SARS-COV-2 neutralising antibodies	~15 min	[63]
3	Soluble Extracellular	Fluorescence	SARS-COV-2 neutralising antibodies	18 min per test, 40 min for 20 tests	[64]
4	Soluble Extracellular	Fluorescence	SARS-COV-2 drug screening and neutralising antibodies	20 min	[65]
5	Not Stated	Fluorescence	SARS-COV-2 neutralising antibodies	~5 min	[66]

Biosensors for the detection of SARS-CoV-2 neutralising antibodies or anti-SARS-CoV-2 drugs typically operate as a competitive assay, where they measure the ability of an antibody or drug candidates to prevent the binding of SARS-CoV-2 S protein/S1/RBD [30, 63, 64]. One

example of a lateral flow approach is using europium nanoparticle labelled RBD, which does not bind to the ACE2 test line if neutralising antibodies are present. This test also includes an additional test line using immobilised anti-human-Fc antibodies, which capture and detect any labelled RBD attached to neutralising human antibodies as an extra verification [63].

The use of ACE2 instead of antibodies on a lateral flow test strip together with a labelled antibody probe can also create a dual-purpose sensor that can detect both neutralising antibodies and SARS-CoV-2 (as shown previously in Figure 2A2). For neutralising antibody detection, RBD was added to the conjugation mixture, creating a competitive sensor. The presence of neutralising antibodies in the sample prevents the binding and detection by the labelled antibody-RBD conjugate at the ACE2 line [30]. This allows the same test strip to detect both viruses and neutralising antibodies in a dual-use sensor.

Fluorescence sensors for neutralising antibody or anti-SARS-CoV-2 drug detection often rely on the detection of fluorescent RBD or S1 attached to ACE2 conjugated to a surface such as magnetic nanoparticles [65] or a glass probe [64]. The presence of a neutralising antibody or anti-SARS-CoV-2 drug prevents the fluorescent RBD/S1 binding to the ACE2 and result in a reduced fluorescence on the nanoparticle or probe. An alternative “light on” SARS-CoV-2 neutralising antibody detection makes use of FRET between an RBD conjugated fluorescent nanoparticle and ACE2 conjugated quenching nanoparticle [66], where the presence of the neutralising antibody prevents fluorescent nanoparticle from binding to the quencher and results in the solution remaining fluorescent.

7. Performance comparison

For a biosensor to be clinically viable, the LOD (a measure of analytical sensitivity) must be relevant to the analyte concentration of clinical samples. Biosensor LODs are typically viral LODs (using SARS-CoV-2 virus or pseudoviruses) or protein LODs (using S protein, S1 or RBD). Viral LODs are typically reported either in PCR units describing RNA/DNA copies/ml or infective units ($TCID_{50}$/ml or PFU/ml), depending on if PCR or culture methods were used to benchmark the biosensor's LOD. Protein LODs are quoted in mass/molar units (e.g., ng/ml or nM). An LOD of about 10^6 copies/ml for ART kits is acceptable by the world health organisation as this LOD corresponds to the viral load of individuals with a high viral load [67]. Although ART kits do not detect viral RNA or viral viability, the LOD quoted for these ART kits is typically stated in copies/ml [68], PFU/ml or $TCID_{50}$/ml [69]. These units are used as PCR [7, 68] or culture based methods are used often used to benchmark the ART kits performance [69, 70]. Additionally, for the test to be acceptable by regulatory bodies such as the FDA, the test must fulfil various parameters, i.e. selectivity, selectivity, accuracy, precision, recovery and stability etc. [71]. Most of the ACE2-based optical biosensors showcased in this review are at pre-clinical stages of development and hence much of this data is unavailable.

As seen from Tables 1 and 2, the reported viral LOD for the lateral flow [38], colorimetric [62] and fluorescence [26] is in range of ~10^5 - 10^6 copies/ml of inactivated SARS-CoV-2 or pseudovirus. This LOD range is similar to that of the commercially available ART kits of 10^6 – 10^7 copies/ml [7], and meets the LOD values recommended by the World Health Organisation of 10^6 copies/ml for ART tests [67]. Two SERS biosensors [35, 37] also reported a LOD below that of current commercial RT-PCRs (10^2 – 10^3 copies/ml) [3, 26]. While electrochemical biosensors based on ACE2 can also achieve very low LODs, (e.g. 38.6 copies/ml) [57], electrochemical biosensors are vulnerable to interference from electrochemically active media or sample

contaminants [72] which can affect their accuracy especially at low analyte concentrations. These reported LOD values show the ACE2 derived biosensors can be comparable with or exceed that of currently approved systems.

As discussed previously in Section 3, due to the difficulty in handling viable SARS-CoV-2 viruses, many biosensors report their performance (e.g., LOD) using protein surrogates. However, it can be difficult to determine the clinical performance of a biosensor compared to the accepted PCR standard (i.e., virus copies/ml) based on the LOD of a surrogate system (e.g., nM of S protein). The differences in structural and chemical properties between entire virions and isolated virus proteins are likely to affect different biosensor designs differently. For example, the colorimetric ACE2 mimic sensor developed by Zhu et al [62], that reported a SARS-CoV-2 RBD LOD of 0.01nM, and the ACE2 mimic FRET-based biosensor by Tripathy, S. P et al., [26], that reported a SARS-CoV-2 RBD LOD at 700 aM. Both biosensors reported an identical viral LOD of 10^5 Copies/ml of SARS-CoV-2 peudovirus [26, 62]. Hence, while biosensors may report highly sensitive detection of S protein/S1/RBD, care must be taken when attempting to extrapolate the viral LOD performance of these biosensors from their protein LOD values.

In addition to analytical sensitivity, assay time is also important for rapid detection of SARS-CoV-2 infections. From Tables 1 and 2, the assay time for biosensors using ACE2 or ACE2 mimics ranges from 3 minutes [42] to 120 minutes [73] per sample, with a median value of 20 minutes, which are significantly faster than conventional PCR testing. Additionally, many of the biosensors are portable, such as lateral flow strips [38] and portable Raman spectrophotometers [37], and are capable of point-of-care diagnosis of COVID19.

There is also potential for these biosensors to be used for environmental surveillance of SARS-CoV-2. For instance, the concentration of airborne SARS-CoV-2 in indoor settings with

infected individuals can reach up to 3.38×10^3 copies/m^3 [74]. It is possible to adapt low LOD biosensors to detect the presence of the virus in environmental samples by combining the biosensor with a suitable sampling method. For example, a biosensor combined with an electrostatic air sampler was developed for the detection of influenza and coronaviruses [75].

8. Conclusion and future perspective

In this review, optical biosensors using ACE2 and ACE2 mimics as the affinity ligand were reviewed for their applications of detecting coronaviruses infection and for detecting neutralising antibodies or as a screen for anti-SARS-CoV-2 drugs. ACE2 mimics, i.e., the short peptides from ACE2 involved in the binding to the SARS-CoV-2 S protein, are alternative to ACE2 protein for biosensor designs and can support the development of novel biosensors of various formats where the larger ACE2 protein is unsuitable such as FRET or direct SERS biosensors. Additionally, ACE2 mimics peptides are selective to the SARS-CoV-2 virus over SARS-CoV-1 due to differences in the residues involved in S protein binding. While some ACE2 optical biosensors have been tested against SARS-CoV-2 samples from patient swabs [28, 37, 38, 40], many ACE2 based optical biosensors use viral proteins as safe surrogates for performance testing. which is difficult to correlate with a viral LOD (i.e., SARS-CoV-2 virus or pseudovirus) to determine the sensor's clinical suitability. This difficulty in handling live virus containing clinical swab samples is a bottleneck in the development of ACE2 based SARS-CoV-2 biosensors, as compared to, for example virus inactivated clinical serum samples for serological tests [76]. This bottleneck can be alleviated by increasing the accessibility of clinical samples from BSL3 facilities to researchers, for example, by establishing dedicated groups or centres to facilitate such clinical sample testing. While biosensors are in development, it is important to consult the published guidelines from the

relevant regulatory body for the design of experiments to validate the biosensor. This would allow for easier regulatory approval and a more rapid adoption of the biosensor.

As the COVID-19 pandemic enters its fourth year and continues to affect the world, the relatively rapid turnover time of biosensors as well as the potential for on-site diagnosis make them an indispensable tool in limiting the effects of the disease. The use of ACE2 or ACE2 mimics in biosensors futureproofs the sensor to new mutants of the virus as long as the virus S protein still utilises ACE2. These ACE2 mimics can be further modified to improve their binding affinity to the S protein [25]. Additionally, the recent advancement in machine-learning and data processing capabilities can further increase the speed and accuracy of certain biosensors, for example, processing complex Raman spectra for SERS based fingerprinting sensors to identify binding of viruses [35] as mentioned in Section 4.3. When optical biosensors have multiple output signals, AI algorithm can assist the classification of the detection outcome, as demonstrated recently for wound healing monitoring [77]. Such AI-enabled multichannel optical sensors can be developed for detecting SARS-CoV-2 variants of concerns and the emerging of new strains. With all the earlier mentioned technological elements, cell receptor- or receptor mimic-based optical biosensors can be developed for any pathogen that utilises a known receptor, enabling the creation of biosensors that are resistant to future mutations of the pathogen. We hope this review can inspire for the further translation of such receptor-based optical biosensor technologies into novel COVID-19 detection kits, as well as to expand their development to detect other future pathogens.

Declaration of conflicts of interest

The authors declare that there are no known competing personal or financial conflicts of interest regarding this publication.

Acknowledgements

Funding: This work was supported by the Programme for Research in Epidemic Preparedness and Response (PREPARE), under the Ministry of Health, Singapore. [Grant reference number: PREPARE-CS1-2022-003].

References

[1] Z. Ke, J. Oton, K. Qu, M. Cortese, V. Zila, L. McKeane, T. Nakane, J. Zivanov, C.J. Neufeldt, B. Cerikan, J.M. Lu, J. Peukes, X. Xiong, H.-G. Kräusslich, S.H.W. Scheres, R. Bartenschlager, J.A.G. Briggs, Nature 588 (2020) 498.
[2] Y.R. Guo, Q.D. Cao, Z.S. Hong, Y.Y. Tan, S.D. Chen, H.J. Jin, K.S. Tan, D.Y. Wang, Y. Yan, Mil Med Res 7 (2020) 11.
[3] P. Pokhrel, C. Hu, H. Mao, ACS Sensors 5 (2020) 2283.
[4] H. Gremmels, B.M.F. Winkel, R. Schuurman, A. Rosingh, N.A.M. Rigter, O. Rodriguez, J. Ubijaan, A.M.J. Wensing, M.J.M. Bonten, L.M. Hofstra, EClinicalMedicine 31 (2021) 100677.
[5] L.E. Brümmer, S. Katzenschlager, M. Gaeddert, C. Erdmann, S. Schmitz, M. Bota, M. Grilli, J. Larmann, M.A. Weigand, N.R. Pollock, A. Macé, S. Carmona, S. Ongarello, J.A. Sacks, C.M. Denkinger, PLOS Medicine 18 (2021) e1003735.
[6] W.-Y. Hsieh, C.-H. Lin, T.-C. Lin, C.-H. Lin, H.-F. Chang, C.-H. Tsai, H.-T. Wu, C.-S. Lin, Diagnostics 11 (2021) 1760.
[7] V.M. Corman, V.C. Haage, T. Bleicker, M.L. Schmidt, B. Mühlemann, M. Zuchowski, W.K. Jo, P. Tscheak, E. Möncke-Buchner, M.A. Müller, A. Krumbholz, J.F. Drexler, C. Drosten, The Lancet Microbe 2 (2021) e311.
[8] R. Wölfel, V.M. Corman, W. Guggemos, M. Seilmaier, S. Zange, M.A. Müller, D. Niemeyer, T.C. Jones, P. Vollmar, C. Rothe, M. Hoelscher, T. Bleicker, S. Brünink, J. Schneider, R. Ehmann, K. Zwirglmaier, C. Drosten, C. Wendtner, Nature 581 (2020) 465.
[9] B. Nagel, H. Dellweg, L.M. Gierasch, Pure and Applied Chemistry 64 (1992) 143.
[10] A.K. Singh, S. Mittal, M. Das, A. Saharia, M. Tiwari, Alexandria Engineering Journal 67 (2023) 673.
[11] E. Mahase, BMJ 377 (2022) o1009.
[12] R. Mungmunpuntipantip, V. Wiwanitkit, Int J Physiol Pathophysiol Pharmacol 14 (2022) 124.
[13] G. Moreira, L. Casso-Hartmann, S.P.A. Datta, D. Dean, E. McLamore, D. Vanegas, Frontiers in Sensors 3 (2022).
[14] G. Karuppaiah, A. Vashist, M. Nair, M. Veerapandian, P. Manickam, Biosensors and Bioelectronics: X 13 (2023) 100324.
[15] M. Mostafa, A. Barhoum, E. Sehit, H. Gewaid, E. Mostafa, M.M. Omran, M.S. Abdalla, F.M. Abdel-Haleem, Z. Altintas, R.J. Forster, TrAC Trends in Analytical Chemistry 157 (2022) 116750.
[16] S. Alsalameh, K. Alnajjar, T. Makhzoum, N. Al Eman, I. Shakir, T.A. Mir, K. Alkattan, R. Chinnappan, A. Yaqinuddin, Biosensors 12 (2022) 898.
[17] L. Tessaro, A. Aquino, P. Panzenhagen, N. Joshi, C.A. Conte-Junior, Journal of Pharmaceutical and Biomedical Analysis 222 (2023) 115087.
[18] B.A. Taha, Y. Al Mashhadany, Q. Al-Jubouri, A.R.B.A. Rashid, Y. Luo, Z. Chen, S. Rustagi, V. Chaudhary, N. Arsad, Science of The Total Environment 880 (2023) 163333.

[19] I. Gul, S. Zhai, X. Zhong, Q. Chen, X. Yuan, Z. Du, Z. Chen, M.A. Raheem, L. Deng, E. Leeansyah, C. Zhang, D. Yu, P. Qin, Biosensors 12 (2022) 984.
[20] H. Wei, C. Zhang, X. Du, Z. Zhang, Talanta 251 (2023) 123813.
[21] S.M. Gonzalez, A.B. Siddik, R.-C. Su, Frontiers in Immunology 12 (2021).
[22] R. Yan, Y. Zhang, Y. Li, L. Xia, Y. Guo, Q. Zhou, Science 367 (2020) 1444.
[23] H.L. Svilenov, F. Delhommel, T. Siebenmorgen, F. Rührnößl, G.M. Popowicz, A. Reiter, M. Sattler, C. Brockmeyer, J. Buchner, Communications Biology 6 (2023) 386.
[24] B. Kang, Y. Lee, J. Lim, D. Yong, Y. Ki Choi, S. Woo Yoon, S. Seo, S. Jang, S. Uk Son, T. Kang, J. Jung, K.-S. Lee, M.H. Kim, E.-K. Lim, Chemical Engineering Journal 442 (2022) 136143.
[25] S. Paul, S. Nadendla, M.E. Sobhia, The Journal of Physical Chemistry Letters 13 (2022) 7420.
[26] S.P. Tripathy, M. Ponnapati, S. Bhat, J. Jacobson, P. Chatterjee, Science Advances 8 (2022) eabn2378.
[27] T.D. Payne, S.J. Klawa, T. Jian, S.H. Kim, M.J. Papanikolas, R. Freeman, Z.D. Schultz, ACS Sensors 6 (2021) 3436.
[28] D. Soto, J. Orozco, Analytica Chimica Acta 1205 (2022) 339739.
[29] C.W. Tan, W.N. Chia, X. Qin, P. Liu, M.I.C. Chen, C. Tiu, Z. Hu, V.C.-W. Chen, B.E. Young, W.R. Sia, Y.-J. Tan, R. Foo, Y. Yi, D.C. Lye, D.E. Anderson, L.-F. Wang, Nature Biotechnology 38 (2020) 1073.
[30] J.-H. Lee, Y. Lee, S.K. Lee, J. Kim, C.-S. Lee, N.H. Kim, H.G. Kim, Biosensors and Bioelectronics 203 (2022) 114034.
[31] A.L. Ferreira, L.F. de Lima, M.D.T. Torres, W.R. de Araujo, C. de la Fuente-Nunez, ACS Nano 15 (2021) 17453.
[32] Y.T. Büyüksünetçi, B.E. Çitil, U. Tapan, Ü. Anık, Microchimica Acta 188 (2021) 335.
[33] R.L. Pinals, F. Ledesma, D. Yang, N. Navarro, S. Jeong, J.E. Pak, L. Kuo, Y.-C. Chuang, Y.-W. Cheng, H.-Y. Sun, M.P. Landry, Nano Letters 21 (2021) 2272.
[34] C. Huang, Z. Tan, K. Zhao, W. Zou, H. Wang, H. Gao, S. Sun, D. Bu, W. Chai, Y. Li, iScience 24 (2021) 103272.
[35] Y. Yang, Y. Peng, C. Lin, L. Long, J. Hu, J. He, H. Zeng, Z. Huang, Z.-Y. Li, M. Tanemura, J. Shi, J.R. Lombardi, X. Luo, Nano-Micro Letters 13 (2021) 109.
[36] P. Ge, J. Tsao, S. Schein, T.J. Green, M. Luo, Z.H. Zhou, Science 327 (2010) 689.
[37] Y. Li, C. Lin, Y. Peng, J. He, Y. Yang, Sensors and Actuators B: Chemical 365 (2022) 131974.
[38] J.-H. Lee, M. Choi, Y. Jung, S.K. Lee, C.-S. Lee, J. Kim, J. Kim, N.H. Kim, B.-T. Kim, H.G. Kim, Biosensors and Bioelectronics 171 (2021) 112715.
[39] O.J. Achadu, N. Nwaji, D. Lee, J. Lee, E.M. Akinoglu, M. Giersig, E.Y. Park, Nanoscale Advances 4 (2022) 871.
[40] G. Rong, Y. Zheng, X. Li, M. Guo, Y. Su, S. Bian, B. Dang, Y. Chen, Y. Zhang, L. Shen, H. Jin, R. Yan, L. Wen, P. Zhu, M. Sawan, Biosensors and Bioelectronics 220 (2023) 114861.
[41] Y. Yang, J. Murray, J. Haverstick, R.A. Tripp, Y. Zhao, Sensors and Actuators B: Chemical 359 (2022) 131604.
[42] J. Han, S.-L. Lee, J. Kim, G. Seo, Y.W. Lee, Microchimica Acta 189 (2022) 321.
[43] J. He, S. Zhu, J. Zhou, W. Jiang, L. Yin, L. Su, X. Zhang, Q. Chen, X. Li, Frontiers in Bioengineering and Biotechnology 10 (2023).
[44] Y. Zhang, Y. Chai, Z. Hu, Z. Xu, M. Li, X. Chen, C. Yang, J. Liu, Frontiers in Bioengineering and Biotechnology 10 (2022).
[45] G.Y. Ang, K.G. Chan, C.Y. Yean, C.Y. Yu, Diagnostics 12 (2022) 2854.
[46] Y. Liu, L. Zhan, J.W. Shen, B. Baro, A. Alemany, J. Sackrison, O. Mitjà, J.C. Bischof, ACS Applied Nano Materials 4 (2021) 13826.
[47] J. Budd, B.S. Miller, N.E. Weckman, D. Cherkaoui, D. Huang, A.T. Decruz, N. Fongwen, G.-R. Han, M. Broto, C.S. Estcourt, J. Gibbs, D. Pillay, P. Sonnenberg, R. Meurant, M.R. Thomas, N. Keegan, M.M.

Stevens, E. Nastouli, E.J. Topol, A.M. Johnson, M. Shahmanesh, A. Ozcan, J.J. Collins, M. Fernandez Suarez, B. Rodriguez, R.W. Peeling, R.A. McKendry, Nature Reviews Bioengineering 1 (2023) 13.
[48] P. Forssén, J. Samuelsson, K. Lacki, T. Fornstedt, Analytical Chemistry 92 (2020) 11520.
[49] B.D. Ventura, M. Cennamo, A. Minopoli, R. Campanile, S.B. Censi, D. Terracciano, G. Portella, R. Velotta, ACS Sensors 5 (2020) 3043.
[50] J. Zhang, T. Xiao, Y. Cai, B. Chen, Current Opinion in Virology 50 (2021) 173.
[51] T. Meirson, D. Bomze, G. Markel, Bioinformatics 37 (2020) 929.
[52] A.S. De Silva Indrasekara, Journal of Applied Physics 129 (2021).
[53] I. Jung, M. Kim, M. Kwak, G. Kim, M. Jang, S.M. Kim, D.J. Park, S. Park, Nature Communications 9 (2018) 1010.
[54] H. Hofmann, K. Pyrc, L. van der Hoek, M. Geier, B. Berkhout, S. Pöhlmann, Proceedings of the National Academy of Sciences 102 (2005) 7988.
[55] D. Buratto, A. Saxena, Q. Ji, G. Yang, S. Pantano, F. Zonta, Frontiers in Immunology 12 (2021).
[56] A.C. Mathewson, A. Bishop, Y. Yao, F. Kemp, J. Ren, H. Chen, X. Xu, B. Berkhout, L. van der Hoek, I.M. Jones, J Gen Virol 89 (2008) 2741.
[57] V.J. Vezza, A. Butterworth, P. Lasserre, E.O. Blair, A. MacDonald, S. Hannah, C. Rinaldi, P.A. Hoskisson, A.C. Ward, A. Longmuir, S. Setford, E.C.W. Farmer, M.E. Murphy, D.K. Corrigan, Chemical Communications 57 (2021) 3704.
[58] P. Towler, B. Staker, S.G. Prasad, S. Menon, J. Tang, T. Parsons, D. Ryan, M. Fisher, D. Williams, N.A. Dales, M.A. Patane, M.W. Pantoliano, Journal of Biological Chemistry 279 (2004) 17996.
[59] P.A. Santana, C.A. Álvarez, S. Valenzuela, A. Manchego, F. Guzmán, C. Tirapegui, M. Ahumada, Biosensors 13 (2023) 473.
[60] A. Ali, R. Vijayan, Scientific Reports 10 (2020) 14214.
[61] K. Wu, W. Li, G. Peng, F. Li, Proceedings of the National Academy of Sciences 106 (2009) 19970.
[62] Q. Zhu, X. Zhou, Journal of Hazardous Materials 425 (2022) 127923.
[63] X. Duan, Y. Shi, X. Zhang, X. Ge, R. Fan, J. Guo, Y. Li, G. Li, Y. Ding, R.A. Osman, W. Jiang, J. Sun, X. Luan, G. Zhang, Biosensors and Bioelectronics 199 (2022) 113883.
[64] H.S. Yang, S.E. Racine-Brzostek, M. Karbaschi, J. Yee, A. Dillard, P.A.D. Steel, W.T. Lee, K.A. McDonough, Y. Qiu, T.J. Ketas, E. Francomano, P.J. Klasse, L. Hatem, L. Westblade, H. Wu, H. Chen, R. Zuk, H. Tan, R.C. Girardin, A.P. Dupuis, A.F. Payne, J.P. Moore, M.M. Cushing, A. Chadburn, Z. Zhao, Biosensors and Bioelectronics 178 (2021) 113008.
[65] S. Roth, A. Danielli, Sensors 21 (2021) 4814.
[66] L. Zhao, Q. Song, W. Mai, M. Deng, Y. Lei, L. Chen, W. Kong, L. Zhang, L. Zhang, Y. Li, H. Ye, Y. Qin, T. Zhang, Y. Hu, T. Ji, W. Wei, Chemical Engineering Journal 468 (2023) 143616.
[67] A.I. Cubas-Atienzar, K. Kontogianni, T. Edwards, D. Wooding, K. Buist, C.R. Thompson, C.T. Williams, E.I. Patterson, G.L. Hughes, L. Baldwin, C. Escadafal, J.A. Sacks, E.R. Adams, Scientific Reports 11 (2021) 18313.
[68] A. Osterman, I. Badell, E. Basara, M. Stern, F. Kriesel, M. Eletreby, G.N. Öztan, M. Huber, H. Autenrieth, R. Knabe, P.M. Späth, M. Muenchhoff, A. Graf, S. Krebs, H. Blum, J. Durner, L. Czibere, C. Dächert, L. Kaderali, H.-M. Baldauf, O.T. Keppler, Medical Microbiology and Immunology 211 (2022) 105.
[69] T. Peto, D. Affron, B. Afrough, A. Agasu, M. Ainsworth, A. Allanson, K. Allen, C. Allen, L. Archer, N. Ashbridge, I. Aurfan, M. Avery, E. Badenoch, P. Bagga, R. Balaji, E. Baldwin, S. Barraclough, C. Beane, J. Bell, T. Benford, S. Bird, M. Bishop, A. Bloss, R. Body, R. Boulton, A. Bown, C. Bratten, C. Bridgeman, D. Britton, T. Brooks, M. Broughton-Smith, P. Brown, B. Buck, E. Butcher, W. Byrne, G. Calderon, S. Campbell, O. Carr, P. Carter, D. Carter, M. Cathrall, M. Catton, J. Chadwick, D. Chapman, K.K. Chau, T. Chaudary, S. Chidavaenzi, S. Chilcott, B. Choi, H. Claasen, S. Clark, R. Clarke, D. Clarke, R. Clayton, K. Collins, R. Colston, J. Connolly, E. Cook, M. Corcoran, B. Corley, L. Costello, C. Coulson, A. Crook, D.W. Crook, S. D'Arcangelo, M.-A. Darby, J. Davis, R. de Koning, P. Derbyshire, P. Devall, M. Dolman, N.

Draper, M. Driver, S. Dyas, E. Eaton, J. Edwards, R. Elderfield, K. Ellis, G. Ellis, S. Elwell, R. Evans, B. Evans, M. Evans, R. Evans, D. Eyre, C. Fahey, V. Fenech, J. Field, A. Field, T. Foord, T. Fowler, M. French, H. Fuchs, J. Gan, J. Gernon, G. Ghadiali, N. Ghuman, K. Gibbons, G. Gill, K. Gilmour, A. Goel, S. Gordon, T. Graham, A. Grassam-Rowe, D. Green, A. Gronert, T. Gumsley-Read, C. Hall, B. Hallis, S. Hammond, P. Hammond, B. Hanney, V. Hardy, G. Harker, A. Harris, M. Havinden-Williams, E. Hazell, J. Henry, K. Hicklin, K. Hollier, B. Holloway, S.J. Hoosdally, S. Hopkins, L. Hughes, S. Hurdowar, S.-A. Hurford, J. Jackman, H. Jackson, R. Johns, S. Johnston, J. Jones, T. Kanyowa, K. Keating-Fedders, S. Kempson, I. Khan, B. Khulusi, T. Knight, A. Krishna, P. Lahert, Z. Lampshire, D. Lasserson, K. Lee, L.Y.W. Lee, A. Legard, C. Leggio, J. Liu, T. Lockett, C. Logue, V. Lucas, S.F. Lumley, V. Maripuri, D. Markham, E. Marshall, P.C. Matthews, S. McKee, D.F. McKee, N. McLeod, A. McNulty, F. Mellor, R. Michel, A. Mighiu, J. Miller, Z. Mirza, H. Mistry, J. Mitchell, M.E. Moeser, S. Moore, A. Muthuswamy, D. Myers, G. Nanson, M. Newbury, S. Nicol, H. Nuttall, J.J. Nwanaforo, L. Oliver, W. Osbourne, J. Osbourne, A. Otter, J. Owen, S. Panchalingam, D. Papoulidis, J.D. Pavon, A. Peace, K. Pearson, L. Peck, A. Pegg, S. Pegler, H. Permain, P. Perumal, L. Peto, T.E.A. Peto, T. Pham, H.L. Pickford, M. Pinkerton, M. Platton, A. Price, E. Protheroe, H. Purnell, L. Rawden, S. Read, C. Reynard, S. Ridge, T.G. Ritter, J. Robinson, P. Robinson, G. Rodger, C. Rowe, B. Rowell, A. Rowlands, S. Sampson, K. Saunders, R. Sayers, J. Sears, R. Sedgewick, L. Seeney, A. Selassie, L. Shail, J. Shallcross, L. Sheppard, A. Sherkat, S. Siddiqui, A. Sienkiewicz, L. Sinha, J. Smith, E. Smith, E. Stanton, T. Starkey, A. Stawiarski, A. Sterry, J. Stevens, M. Stockbridge, N. Stoesser, A. Sukumaran, A. Sweed, S. Tatar, H. Thomas, C. Tibbins, S. Tiley, J. Timmins, C. Tomas-Smith, O. Topping, E. Turek, T. Neibler, K. Trigg-Hogarth, E. Truelove, C. Turnbull, D. Tyrrell, A. Vaughan, J. Vertannes, R. Vipond, L. Wagstaff, J. Waldron, P. Walker, A.S. Walker, M. Walters, J.Y. Wang, E. Watson, K. Webberley, K. Webster, G. Westland, I. Wickens, J. Willcocks, H. Willis, S. Wilson, B. Wilson, L. Woodhead, D. Wright, B. Xavier, F. Yelnoorkar, L. Zeidan, R. Zinyama, EClinicalMedicine 36 (2021) 100924.

[70] P.N. Levett, B. Cheung, J. Kustra, T. Pidduck, A. Mak, F. Tsang, M. Petric, M. Krajden, J Clin Virol 142 (2021) 104938.

[71] U.S. Department of Health and Human Services; Food and Drug Administration, Bioanalytical Method Validation Guidance for Industry. https://www.fda.gov/, 2018.

[72] M. Mehrvar, M. Abdi, Analytical Sciences 20 (2004) 1113.

[73] D. Beduk, J. Ilton de Oliveira Filho, T. Beduk, D. Harmanci, F. Zihnioglu, C. Cicek, R. Sertoz, B. Arda, T. Goksel, K. Turhan, K.N. Salama, S. Timur, Biosensors and Bioelectronics: X 10 (2022) 100105.

[74] P.Y. Chia, K.K. Coleman, Y.K. Tan, S.W.X. Ong, M. Gum, S.K. Lau, X.F. Lim, A.S. Lim, S. Sutjipto, P.H. Lee, T.T. Son, B.E. Young, D.K. Milton, G.C. Gray, S. Schuster, T. Barkham, P.P. De, S. Vasoo, M. Chan, B.S.P. Ang, B.H. Tan, Y.-S. Leo, O.-T. Ng, M.S.Y. Wong, K. Marimuthu, D.C. Lye, P.L. Lim, C.C. Lee, L.M. Ling, L. Lee, T.H. Lee, C.S. Wong, S. Sadarangani, R.J. Lin, D.H.L. Ng, M. Sadasiv, T.W. Yeo, C.Y. Choy, G.S.E. Tan, F. Dimatatac, I.F. Santos, C.J. Go, Y.K. Chan, J.Y. Tay, J.Y.-L. Tan, N. Pandit, B.C.H. Ho, S. Mendis, Y.Y.C. Chen, M.Y. Abdad, D. Moses, T. for the Singapore Novel Coronavirus Outbreak Research, Nature Communications 11 (2020) 2800.

[75] H.R. Kim, S. An, J. Hwang, Biosensors and Bioelectronics 170 (2020) 112656.

[76] T.T.S. Lew, K.M.M. Aung, S.Y. Ow, S.N. Amrun, L. Sutarlie, L.F.P. Ng, X. Su, ACS Nano 15 (2021) 12286.

[77] X.T. Zheng, Z. Yang, L. Sutarlie, M. Thangaveloo, Y. Yu, N.A.B.M. Salleh, J.S. Chin, Z. Xiong, D.L. Becker, X.J. Loh, B.C.K. Tee, X. Su, Science Advances 9 (2023) eadg6670.